Diagnosing momentum and vorticity budgets in MOM6

Hemant Khatri[1] and Stephen M. Griffies[2]

Draft from July 7, 2021

Abstract

These notes discuss the discrete velocity equations of MOM6 and derive the associated vorticity equation. In turn, we document how to diagnose the velocity and vorticity budgets in MOM6, including budgets for depth integrated quantities.

1 Continuous velocity equation

As discussed in Appendix A to *Adcroft et al.* (2019), MOM6 discretizes the vector-invariant velocity equation. This equation takes on the following continuous space-time form using a generalized vertical coordinate $s = s(x, y, z, t)$

$$\left[\frac{\partial \mathbf{u}}{\partial t}\right]_s + \left[\frac{f+\zeta}{h}\right] \hat{\mathbf{z}} \wedge (h\,\mathbf{u}) + w^{(\dot{s})}\,\frac{\partial \mathbf{u}}{\partial z} = -\left[\rho^{-1}\,\nabla_s p + \nabla_s \Phi\right] - \nabla_s K + \boldsymbol{F}^{(\text{horz frict})} + \boldsymbol{F}^{(\text{vert frict})} + \rho^{-1}\,\boldsymbol{\tau}^{(\text{bound})} \tag{1}$$

where we have

$$\boldsymbol{v} = \boldsymbol{u} + \hat{\boldsymbol{z}}\, w = \hat{\boldsymbol{x}}\, u + \hat{\boldsymbol{y}}\, v + \hat{\boldsymbol{z}}\, w \quad \text{velocity} \tag{2}$$

$$\nabla_s = \hat{\boldsymbol{x}} \left[\frac{\partial}{\partial x}\right]_s + \hat{\boldsymbol{y}} \left[\frac{\partial}{\partial y}\right]_s \quad \text{horizontal gradient on } s\text{-surface} \tag{3}$$

$$w^{(\dot{s})} = \frac{\partial z}{\partial s}\frac{\mathrm{D}s}{\mathrm{D}t} \quad \text{dia-surface velocity used for remapping} \tag{4}$$

$$\zeta = \left[\frac{\partial v}{\partial x}\right]_s - \left[\frac{\partial u}{\partial y}\right]_s \quad s\text{-coordinate vertical vorticity} \tag{5}$$

$$\Phi = g\,z \quad \text{geopotential (more complex when have tides)} \tag{6}$$

$$-\rho^{-1}\,\nabla_z p = -\left[\rho^{-1}\,\nabla_s p + \nabla_s \Phi\right] \quad \text{horizontal pressure acceleration} \tag{7}$$

$$K = \frac{u^2 + v^2}{2} \quad \text{horizontal kinetic energy per mass} \tag{8}$$

$$\boldsymbol{F}^{(\text{horz frict})} = \text{horiz friction from horz shear} \quad \text{Laplacian or biharmonic} \tag{9}$$

$$\boldsymbol{F}^{(\text{vert frict})} = \text{vert friction from vertical shear} \quad \text{Laplacian} \tag{10}$$

$$\rho^{-1}\,\boldsymbol{\tau}^{(\text{bound})} = \text{boundary frictional acceleration} \quad \text{wind, bottom drag, etc.} \tag{11}$$

The hydrostatic pressure, p, arises from the weight per horizontal area above a point in the fluid, and it has a boundary condition at the sea surface, $z = \eta(x, y, t)$, set by the pressure applied by the overlying atmosphere and ice, $p(z = \eta) = p_{\text{applied}}$. The external quantities include the vertical component of planetary vorticity $f = 2\Omega \sin\phi$ and the gravitational potential $\Phi = g\,z$. Finally, $\boldsymbol{F}$ is the acceleration due to the divergence of stresses including those provided through boundary interactions.

[1] Hemant.Khatri@noaa.gov, Princeton University AOS Program

[2] Stephen.Griffies@noaa.gov, NOAA Geophysical Fluid Dynamics Laboratory and Princeton University AOS Program

2 Diagnosing terms in the layer velocity equation

In this section we document how to diagnose terms in the MOM6 discretized version of the continuous velocity equation (1). For our purposes, it is sufficient to assume that the velocity equation (1) is discretized in MOM6 by assuming the variables are constant within a grid cell layer according to

$$\boldsymbol{u} \to \boldsymbol{u}_k \qquad h \to h_k \qquad \zeta \to \zeta_k \qquad p \to p_k \qquad \text{etc.}, \tag{12}$$

where k is a cell index that increases downward. MOM6 then provides particular space and time discretizations of accelerations from the local time derivative, Coriolis, nonlinear vorticity, remapping, pressure, friction, boundaries. We are not concerned here with details for how the terms are discretized. Rather, we articulate the diagnostic terms required to close the velocity budget over a grid cell, and to identify where further diagnostics need to be coded.

Table 1 summarizes the layerwise momentum equation diagnostics. For example, for each layer-k we can diagnose the discrete zonal and meridional momentum budgets according to

$$\texttt{dudt} = \texttt{CAu} + \texttt{PFu} + \texttt{u\_BT\_accel} + \texttt{du\_dt\_visc} + \texttt{diffu} + \texttt{remapping(u)} \tag{13a}$$

$$\texttt{dvdt} = \texttt{CAv} + \texttt{PFv} + \texttt{v\_BT\_accel} + \texttt{dv\_dt\_visc} + \texttt{diffv} + \texttt{remapping(v)}. \tag{13b}$$

The remapping terms correspond to the $w^{(\dot{s})}\,\partial_z \boldsymbol{u}$ term in equation (1). They must be diagnosed offline as the residual of the other terms

$$\texttt{remapping(u)} = \texttt{dudt} - \texttt{CAu} - \texttt{PFu} - \texttt{u\_BT\_accel} - \texttt{du\_dt\_visc} - \texttt{diffu} \tag{14a}$$

$$\texttt{remapping(v)} = \texttt{dvdt} - \texttt{CAv} - \texttt{PFv} - \texttt{v\_BT\_accel} - \texttt{dv\_dt\_visc} - \texttt{diffv}. \tag{14b}$$

Relying on offline residual diagnostics is an unsatisfying situation since we ideally want an online diagnostic for each term. Yet we do not understand the MOM6 remapping algorithm sufficiently to compute that diagnostic online and so have settled for an offline residual calculation.[3]

3 Diagnosing terms in the depth-averaged velocity equation

As part of its barotropic time stepping scheme, MOM6 time steps the depth-averaged velocity

$$\overline{\boldsymbol{u}} = \frac{\sum_k h_k \boldsymbol{u}_k}{\sum_k h_k} = \sum_k (h_k/D)\, \boldsymbol{u}_k. \tag{15}$$

For the Boussinesq version of MOM6, h_k is the thickness (in meters) of layer k and

$$D = \sum_k h_k = H(x,y) + \eta(x,y,t) \tag{16}$$

is the total layer thickness from the ocean bottom at $z = -H(x,y)$ to the ocean surface at $z = \eta(x,y,t)$. For the non-Boussinesq version of MOM6, h_k is the mass per horizontal area of a grid cell and D is the total column mass per area (i.e., the bottom pressure minus the applied surface pressure). Our goal is to diagnose terms contributing to the time tendency $\partial_t \overline{\boldsymbol{u}}$.

[3] There is an online diagnostic for the tracer remapping term in MOM6. Nonetheless, the tracer and velocity equation algorithms are distinct, thus making the remapping diagnostics for the tracer equation insufficient to render a diagnostic for the velocity remapping.

MOM6 VELOCITY EQUATION DIAGNOSTICS			
TERM	NAME	DIAGNOSTIC NAME	NOTE
$(\partial \boldsymbol{u}/\partial t)_s$	local time derivative	`dudt`, `dvdt`	
$(\partial \boldsymbol{u}_{bt}/\partial t)_s$	barotropic tendency terms	`ubt_dt`, `vbt_dt`	
$-[(f+\zeta)/h]\hat{\boldsymbol{z}} \wedge (h\,\boldsymbol{u})$ $-\nabla_s K$	linear + nonlinear Coriolis + gradient of kinetic energy	`CAu`, `CAv`	
$-[\zeta/h]\hat{\boldsymbol{z}} \wedge (h\,\boldsymbol{u})$	nonlinear Coriolis	`rvxv`, `rvxu`	
$-\nabla_s K$	gradient of kinetic energy	`gKEu`, `gKEv`	
$-[f/h]\hat{\boldsymbol{z}} \wedge (h\,\boldsymbol{u})$	linear Coriolis	–	diagnose offline from other terms
$w^{(\hat{s})}\,\partial \mathbf{u}/\partial z$	remapping acceleration	–	inferred offline from other terms
$-\left[\rho^{-1}\nabla_s p + \nabla_s \Phi\right]$	pressure acceleration	`PFu`, `PFv`	
	barotropic acceleration	`u_BT_accel`, `v_BT_accel`	contribution from barotropic solver step
$\boldsymbol{F}^{(\text{horz friction})}$	horizontal friction	`diffu`, `diffv`	
$\boldsymbol{F}^{(\text{vert friction})}$ $+\rho^{-1}\,\boldsymbol{\tau}^{(\text{bound, top})}$ $+\rho^{-1}\,\boldsymbol{\tau}^{(\text{bound, bottom})}$	acceleration from vertical friction + acceleration from wind stress + acceleration from bottom stress	`du_dt_visc`, `dv_dt_visc`	
$\rho^{-1}\,\boldsymbol{\tau}^{(\text{bound, top})}$	surface wind stress	`taux`, `tauy`	units of diagnostics are N m^{-2}
$\rho^{-1}\,\boldsymbol{\tau}^{(\text{bound, bottom})}$	bottom boundary stress	`taux_bot`, `tauy_bot`	units of diagnostics are N m^{-2}
$\boldsymbol{F}^{(\text{vert friction})}$	vertical friction	–	diagnose offline from above terms

Table 1: Table of MOM6 velocity equation diagnostic terms. All model diagnosed terms have units of m s^{-2} unless otherwise noted. The barotropic term, which comes from the barotropic time stepping step in MOM6, is required to close the momentum budget. More details on MOM6 diagnostics can be found on mom6.readthedocs.io/en/dev-gfdl/api/generated/pages/Diagnostics.html

3.1 Diagnostic approach

There are two general approaches to diagnosing terms contributing to $\partial_t \overline{\boldsymbol{u}}$. The first approach implements the online diagnostics directly within the MOM6 barotropic time stepping algorithm. However, we do not understand the MOM6 barotropic algorithm sufficiently to be confident in our online diagnostics coded within the algorithm. We thus pursued the following approach, in which we vertically average the layerwise diagnostics from Section 2. An example of the depth average zonal budget is provided in Figure 1, with additional tests of the momentum budgets given in Section A.

3.2 Concerning the time tendency diagnostic

There is one subtlety concerning the $\partial_t \overline{\boldsymbol{u}}$ diagnostic. Namely, the product rule decomposes the time derivative of the depth averaged velocity into two terms [4]

$$\frac{\partial \overline{\boldsymbol{u}}}{\partial t} = \frac{\partial}{\partial t}\left[\sum_k (h_k/D)\,\boldsymbol{u}_k\right] = \left[\sum_k \partial_t(h_k/D)\,\boldsymbol{u}_k + \sum_k (h_k/D)\,\partial_t \boldsymbol{u}_k\right]. \tag{17}$$

The second term on the RHS is the vertical integral of each contribution to $\partial_t \boldsymbol{u}_k$, with the diagnostics listed in Table 1. Furthermore, MOM6 has online diagnostics to perform the fractional-thickness weighting of the RHS terms in equation (17), with these diagnostics listed in Table 2.

However, the first term on the RHS of equation (17) arises from time changes to the relative thickness of a layer, $\partial_t(h_k/D)$, as multiplied by the layer velocity, and this term is not readily diagnosed online in MOM6. So to diagnose $\sum_k \partial_t(h_k/D)\,\boldsymbol{u}_k$, we pursue an indirect method to obtain this term by diagnosing the left hand side of

[4] Hemant: do we compute the fractional thickness with $H(x,y)$ as the static bottom depth, or as $D(x,y,t)$ that includes the time-dependent free surface?
All online thickness-weighted momentum diagnostics use time-varying total depth D.

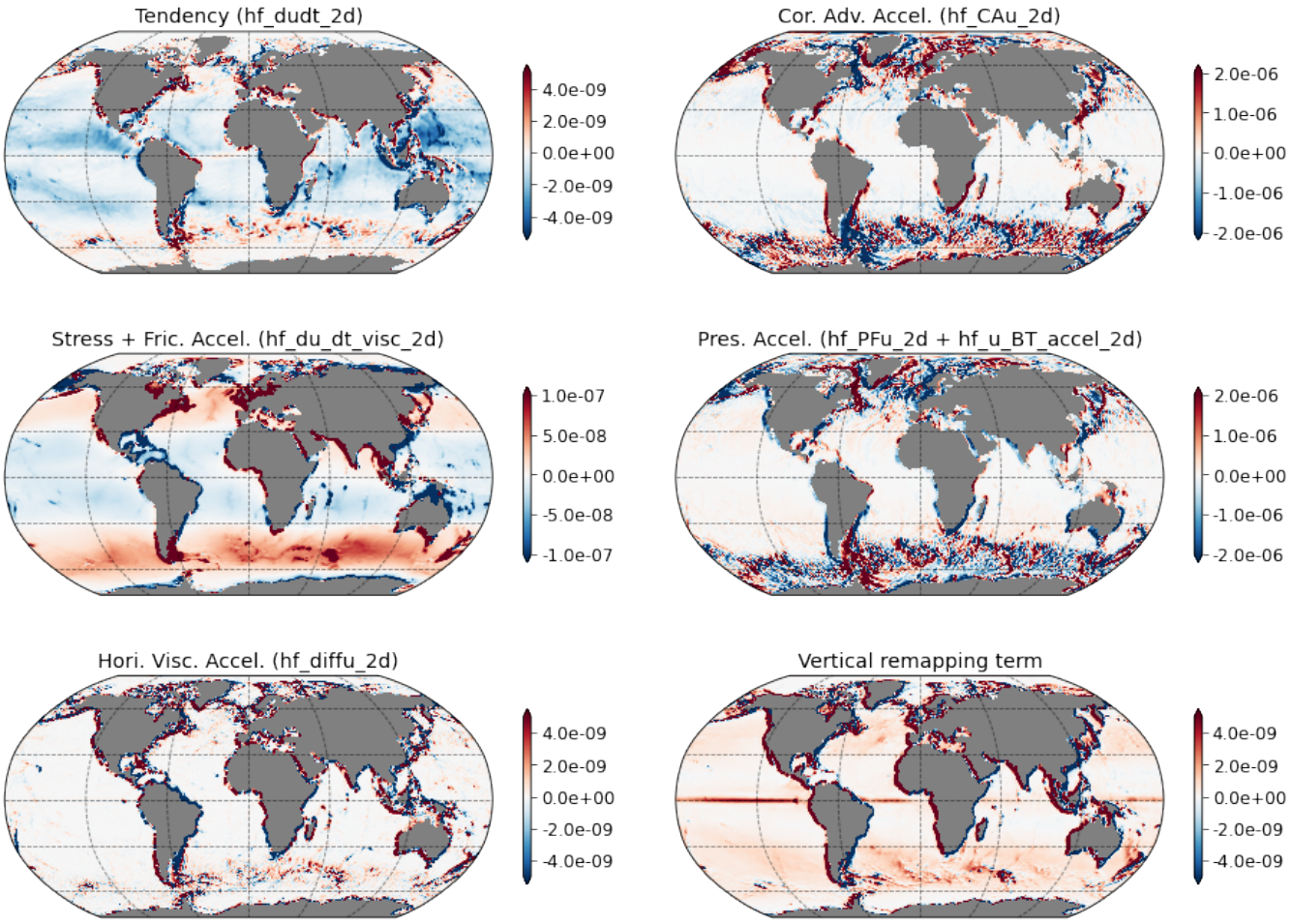

Figure 1: Depth-averaged zonal momentum budget terms (Table 2) from a 1/4° global coupled MOM6 simulation (fields averaged over 5 years). Note the dominance of geostrophy throughout most of the ocean, in which the Coriolis and pressure gradient terms compensate. There is no online diagnostic for the vertical remapping term (lower right panel) in MOM6. Therefore, this term is diagnosed offline as the residual `remapping(u) = hf_dudt_2d − hf_CAu_2d − hf_PFu_2d − hf_u_BT_accel_2d − hf_diffu_2d − hf_du_dt_visc_2d`.

equation (17) according to

$$\frac{\partial \overline{\boldsymbol{u}}}{\partial t} \approx \frac{\overline{\boldsymbol{u}}(\tau+\Delta\tau) - \overline{\boldsymbol{u}}(\tau)}{\Delta\tau}, \tag{18}$$

which requires diagnostic information about both the updated and prior values for the depth-averaged velocity, $\overline{\boldsymbol{u}}$. This time derivative is diagnosed online and saved in

$$\texttt{ubt\_dt} = \partial_t \overline{u} \quad \text{and} \quad \texttt{vbt\_dt} = \partial_t \overline{v}. \tag{19}$$

These diagnosed time tendencies allow us to then perform the offline diagnostic calculation

$$\sum_k \partial_t (h_k/D)\, \boldsymbol{u}_k = \frac{\overline{\boldsymbol{u}}(\tau+\Delta\tau) - \overline{\boldsymbol{u}}(\tau)}{\Delta\tau} - \sum_k (h_k/D)\, \partial_t \boldsymbol{u}_k \tag{20a}$$

$$\sum_k \partial_t (h_k/D)\, u_k = \texttt{ubt\_dt} - \texttt{hf\_dudt\_2d} \tag{20b}$$

$$\sum_k \partial_t (h_k/D)\, v_k = \texttt{vbt\_dt} - \texttt{hf\_dvdt\_2d}. \tag{20c}$$

In Figure 2, we show the left hand side of the zonal equation (20b) as well as the two terms on the RHS.

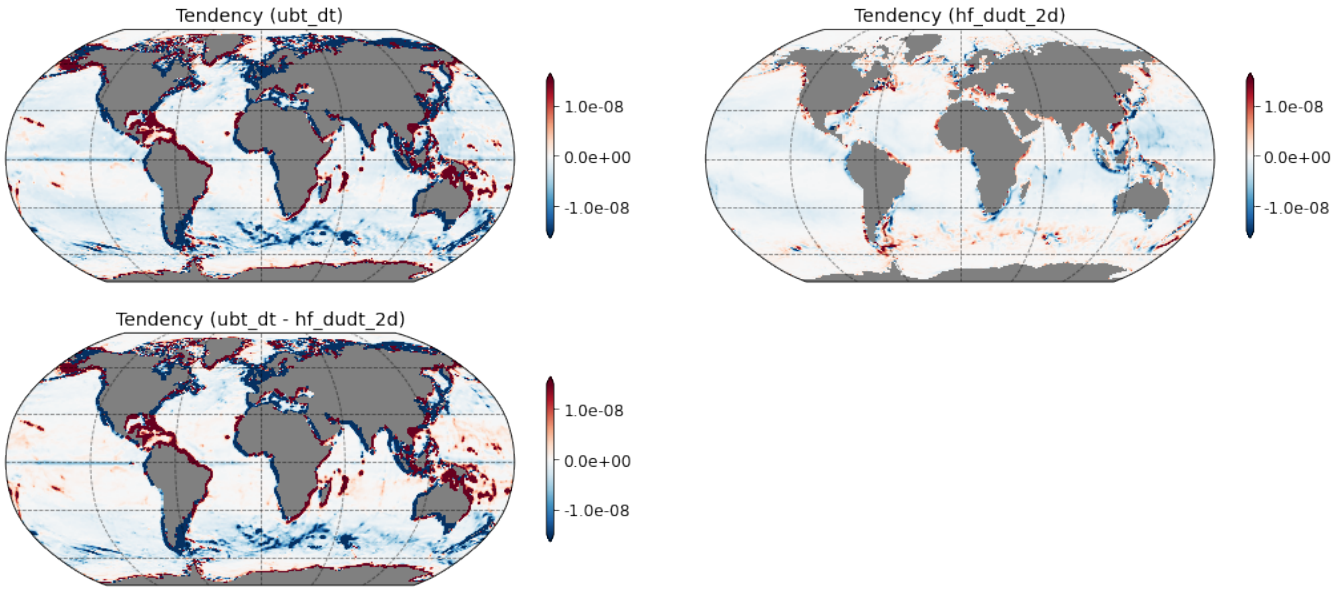

Figure 2: Maps for the terms in equation (20b), with the bottom right panel diagnosed as the difference between the top row. Upper left panel: barotropic velocity tendency; upper right panel: depth averaged velocity tendency; lower left panel: difference. These terms were computed from a 1/4° global coupled MOM6 simulation (fields averaged over 5 years). All fields are spatially smoothed using a Gaussian filter kernel of radius 1°.

4 A general discussion of vorticity budgets

Analysis of the vorticity budget offers useful physical insights into ocean fluid mechanics. For example, theories for the large-scale gyre circulation are based on a study of vorticity. For our purposes here, we are not interested in the vorticity budget for each grid cell in the vertical. Rather, we wish to study budgets for vorticity of a vertical column from the ocean surface to the ocean bottom. This goal can be satisfied in more than one manner, with the following considered here.

1. DEPTH-AVERAGED VORTICITY EQUATION: This budget is obtained by computing the vorticity for each grid cell through taking the curl of the layerwise velocity equation (1). Then, the layerwise vorticity budget is vertically averaged to obtain the depth-averaged vorticity budget.

2. VORTICITY OF THE DEPTH-AVERAGED FLOW: This budget is based on taking the curl of the depth-averaged velocity equation derived from equation (1), which then render terms contributing to the vorticity of the depth-averaged flow.

3. VORTICITY OF THE DEPTH-INTEGRATED FLOW: Here we vertically integrate the velocity equation (1) to compute the budget of depth-integrated flow, and then take the curl to obtain the vorticity budget for the depth-integrated flow.

In the following subsections, we derive the vorticity budget using each of the above approaches and discuss the associated advantages and limitations. We then present the diagnostic approach taken in MOM6.

MOM6 THICKNESS-WEIGHTED VELOCITY EQUATION DIAGNOSTICS		
TERM	NAME	DIAGNOSTIC NAME
$(h/D)(\partial \boldsymbol{u}/\partial t)_s$	Velocity tendency	`hf_dudt`, `hf_dvdt`
$\sum_k (h_k/D)(\partial \boldsymbol{u}_k/\partial t)_s$	Depth mean of velocity tendency	`hf_dudt_2d`, `hf_dvdt_2d`
$-(h/D)\left[[(f+\zeta)/h]\hat{\boldsymbol{z}}\wedge(h\,\boldsymbol{u})+\nabla_s K\right]$	Coriolis + KE gradient	`hf_CAu`, `hf_CAv`
$-\sum_k (h_k/D)\left[[(f+\zeta_k)/h_k]\hat{\boldsymbol{z}}\wedge(h_k\,\boldsymbol{u}_k)+\nabla_s K_k\right]$	Depth mean of Coriolis + KE gradient	`hf_CAu_2d`, `hf_CAv_2d`
$-\sum_k h_k\left[[(f+\zeta_k)/h_k]\hat{\boldsymbol{z}}\wedge(h_k\,\boldsymbol{u}_k)+\nabla_s K_k\right]$	Depth integral of Coriolis + KE gradient	`intz_CAu_2d`, `intz_CAv_2d`
$-(h/D)[\zeta/h]\hat{\boldsymbol{z}}\wedge(h\,\boldsymbol{u})$	Nonlinear Coriolis	`hf_rvxv`, `hf_rvxu`
$-\sum_k (h_k/D)[\zeta_k/h_k]\hat{\boldsymbol{z}}\wedge(h_k\,\boldsymbol{u}_k)$	Depth mean of nonlinear Coriolis	`hf_rvxv_2d`, `hf_rvxu_2d`
$-\sum_k h_k[\zeta_k/h_k]\hat{\boldsymbol{z}}\wedge(h_k\,\boldsymbol{u}_k)$	Depth integral of nonlinear Coriolis	`intz_rvxv_2d`, `intz_rvxu_2d`
$-(h/D)\nabla_s K$	KE gradient	`hf_gKEu`, `hf_gKEv`
$-\sum_k (h_k/D)\nabla_s K_k$	Depth mean of KE gradient	`hf_gKEu_2d`, `hf_gKEv_2d`
$-\sum_k h_k\nabla_s K_k$	Depth integral of KE gradient	`intz_gKEu_2d`, `intz_gKEv_2d`
$-(h/D)\left[\rho^{-1}\nabla_s p+\nabla_s\Phi\right]$	Pressure gradient	`hf_PFu`, `hf_PFv`
$-\sum_k (h_k/D)\left[\rho^{-1}\nabla_s p_k+\nabla_s\Phi_k\right]$	Depth mean of pressure gradient	`hf_PFu_2d`, `hf_PFv_2d`
$-\sum_k h_k\left[\rho^{-1}\nabla_s p_k+\nabla_s\Phi_k\right]$	Depth integral of pressure gradient	`intz_PFu_2d`, `intz_PFv_2d`
	Barotropic acceleration	`hf_u_BT_accel`, `hf_v_BT_accel`
	Depth mean of barotropic accel.	`hf_u_BT_accel_2d`, `hf_v_BT_accel_2d`
	Depth integral of barotropic accel.	`intz_u_BT_accel_2d`, `intz_v_BT_accel_2d`
$(h/D)\boldsymbol{F}^{(\text{horz friction})}$	Horizontal diffusion	`hf_diffu`, `hf_diffv`
$\sum_k (h_k/D)\boldsymbol{F}^{(\text{horz friction})}$	Depth mean of horizontal friction	`hf_diffu_2d`, `hf_diffv_2d`
$\sum_k h_k\boldsymbol{F}^{(\text{horz friction})}$	Depth integral of horizontal friction	`intz_diffu_2d`, `intz_diffv_2d`
$(h/D)\left[\boldsymbol{F}^{(\text{vert friction})}+\rho^{-1}(\boldsymbol{\tau}^{(\text{wind})}+\boldsymbol{\tau}^{(\text{bottom})})\right]$	Acceleration due to vertical friction + wind stress + bottom stress	`hf_du_dt_visc`, `hf_dv_dt_visc`
$\sum_k (h_k/D)\left[\boldsymbol{F}^{(\text{vert friction})}+\rho^{-1}(\boldsymbol{\tau}^{(\text{wind})}+\boldsymbol{\tau}^{(\text{bottom})})\right]$	Depth mean acceleration due to vertical friction + wind stress + bottom stress	`hf_du_dt_visc_2d`, `hf_dv_dt_visc_2d`

Table 2: Table of MOM6 velocity equation diagnostic terms multiplied by fractional layer thicknesses (h_k/D) in units of m s^{-2} as well as when multiplied by the layer thicknesses (h_k) in units of m^2 s^{-2}. The total column thickness is given by $D=\sum_k h_k$, which is time dependent due to movement of the free surface. The sum of all terms with barotropic acceleration terms is required to close the momentum budget. Note that 3D diagnostics are not available for posting in the current MOM6 version, as we see no physical motivation to look at the 3D terms. Rather, they are intermediate terms needed for computing the depth integral. We recommend saving only the depth integrated 2D terms, which have been implemented in MOM6. Nevertheless, the code for posting 3D diagnostics can be found in relevant Fortran files in MOM6 source code as surrounded by comments. For those wishing to save these 3D diagnostics, the comments will need to be removed.

4.1 Depth-averaged vorticity equation

To derive the depth-averaged vorticity budget, we start with the continuous velocity equation (1) written in an abbreviated form and using the Boussinesq approximation

$$\partial_t \mathbf{u} = -f\hat{\mathbf{z}} \wedge \mathbf{u} - \nabla_s(p/\rho_o + \Phi) + (1/\rho_0)\,\partial_z \boldsymbol{\tau} + \mathbf{a} + \mathbf{b} \tag{21a}$$

$$\partial_z \boldsymbol{\tau} = \rho_0 \boldsymbol{F}^{(\text{horz frict})} + \delta(z-\eta)\,\boldsymbol{\tau}^{(\text{top})} - \delta(z+H)\,\boldsymbol{\tau}^{(\text{bot})} \tag{21b}$$

$$\mathbf{a} = -\zeta\,\hat{\mathbf{z}} \wedge \mathbf{u} - \nabla_s K - w^{(\dot{s})}\,\partial_z \mathbf{u} \tag{21c}$$

$$\mathbf{b} = \boldsymbol{F}^{(\text{horz frict})} \tag{21d}$$

$$\zeta = \hat{\boldsymbol{z}} \cdot (\nabla_s \wedge \boldsymbol{u}) \tag{21e}$$

$$\delta(z) = \text{Dirac delta with dimensions } L^{-1}. \tag{21f}$$

The vorticity equation is derived by taking $\hat{\boldsymbol{z}} \cdot \nabla_s \wedge$ of the velocity equation (21a), with a z-coordinate version given by

$$\partial_t \zeta = -v\,\beta + f\partial_z w + \frac{1}{\rho_o} \nabla \wedge \partial_z \boldsymbol{\tau} + \nabla \wedge \mathbf{a} + \nabla \wedge \mathbf{b}, \tag{22}$$

where

$$\beta = \partial_y f \tag{23}$$

is the meridional derivative of the planetary vorticity. Further, we can vertically integrate the vorticity equation (22) and divide by the ocean depth

$$D(x,y,t) = H(x,y) + \eta(x,y,t) \tag{24}$$

to obtain the depth-averaged vorticity budget

$$\langle \partial_t \zeta \rangle = -\beta \langle v \rangle + \frac{f}{D}\left(w^{(\text{top})} - w^{(\text{bot})}\right) + \frac{1}{D\rho_o} \nabla \wedge \left(\boldsymbol{\tau}^{(\text{top})} - \boldsymbol{\tau}^{(\text{bot})}\right) + \langle \nabla \wedge \mathbf{a} \rangle + \langle \nabla \wedge \mathbf{b} \rangle, \tag{25}$$

where

$$\langle m \rangle = \frac{1}{D} \int_{-H}^{\eta} m \, \mathrm{d}z. \tag{26}$$

Further, by applying time-mean (indicated with overbars) and rearranging leads to the time and depth averaged vorticity budget

$$\beta \overline{\langle v \rangle} = \overline{\frac{f}{D}\left(w^{(\text{top})} - w^{(\text{bot})}\right)} + \overline{\frac{1}{D\rho_o} \nabla \wedge \left(\boldsymbol{\tau}^{(\text{top})} - \boldsymbol{\tau}^{(\text{bot})}\right)} + \overline{\langle \nabla \wedge \mathbf{a} \rangle} + \overline{\langle \nabla \wedge \mathbf{b} \rangle} - \overline{\langle \partial_t \zeta \rangle}. \tag{27}$$

The vorticity tendency is typically much smaller than the other terms when taking a sufficiently long time mean.

As seen in equation (27), the depth-averaged meridional flow is affected by several factors. It is required to diagnose individual terms from a model output to assess the relative importance of these terms. However, it is not feasible to use this approach with MOM6 output because diagnostics for terms from depth-averaged vorticity budget are not available. Also, the vertical velocities at the ocean top and bottom are not readily available.

4.2 Vorticity of the depth-averaged flow

Another method to derive vorticity budget is to take the curl of the depth-averaged momentum equation. This approach results in slightly different budget terms than obtained in the method above because depth-averaged vorticity differs from the vorticity of the depth-averaged flow in the presence of variable topography. We first

derive the vorticity equation for the depth-averaged flow and we further discuss the key differences between the approaches. Using equation (21a), the depth-averaged momentum equation is given by

$$\langle \partial_t \mathbf{u} \rangle = -f\,\hat{\mathbf{z}} \wedge \left(\frac{1}{D} \int_{-H}^{\eta} \mathbf{u}\, \mathrm{d}z \right) - \frac{1}{D\rho_o} \int_{-H}^{\eta} \nabla p\, \mathrm{d}z + \frac{1}{D\rho_o} \left(\boldsymbol{\tau}^{(\mathrm{top})} - \boldsymbol{\tau}^{(\mathrm{bot})} \right) + \langle \mathbf{a} \rangle + \langle \mathbf{b} \rangle \tag{28}$$

Since we have taken the depth integral, this equation holds whether in z-coordinates or generalized vertical coordinates, with the only distinction being the specific form of the pressure gradient term and the nonlinear term. We now take the curl of equation (28) to obtain the vorticity equation of the depth-averaged flow

$$\nabla \wedge \langle \partial_t \mathbf{u} \rangle = -\nabla \wedge \left[f\,\hat{\mathbf{z}} \wedge \left(\frac{1}{D} \int_{-H}^{\eta} \mathbf{u}\, \mathrm{d}z \right) \right] - \nabla \wedge \left[\frac{1}{D\rho_o} \int_{-H}^{\eta} \nabla p\, \mathrm{d}z \right] + \nabla \wedge \left[\frac{1}{D\rho_o} \left(\boldsymbol{\tau}^{(\mathrm{top})} - \boldsymbol{\tau}^{(\mathrm{bot})} \right) \right] + \nabla \wedge \langle \mathbf{a} \rangle + \nabla \wedge \langle \mathbf{b} \rangle. \tag{29}$$

With some algebra (note that the Coriolis term is expanded into the first three terms on the RHS below; see details in Section 4.3), the equation can be written

$$\nabla \wedge \langle \partial_t \mathbf{u} \rangle = -\beta \langle v \rangle + f \frac{\langle \mathbf{u} \rangle \cdot \nabla D}{D} + \frac{f}{D} \left(-\frac{Q_m}{\rho_o} + \partial_t \eta \right) - \frac{1}{\rho_o} \nabla \wedge \langle \nabla p \rangle + \nabla \wedge \left[\frac{1}{D\rho_o} \left(\boldsymbol{\tau}^{(\mathrm{top})} - \boldsymbol{\tau}^{(\mathrm{bot})} \right) \right] + \nabla \wedge \langle \mathbf{a} \rangle + \nabla \wedge \langle \mathbf{b} \rangle. \tag{30}$$

Here, Q_m is the mass flux into the ocean on the surface. Application of the time mean operator leads to

$$\beta \overline{\langle v \rangle} = f \frac{\overline{\langle \mathbf{u} \rangle \cdot \nabla D}}{D} - \frac{1}{\rho_o} \nabla \wedge \overline{\langle \nabla p \rangle} - \overline{\frac{f}{D} \frac{Q_m}{\rho_o}} + \overline{\frac{f}{D} \partial_t \eta} - \nabla \wedge \overline{\langle \partial_t \mathbf{u} \rangle} + \overline{\nabla \wedge \left[\frac{1}{D\rho_o} \left(\boldsymbol{\tau}^{(\mathrm{top})} - \boldsymbol{\tau}^{(\mathrm{bot})} \right) \right]} + \nabla \wedge \overline{\langle \mathbf{a} \rangle} + \nabla \wedge \overline{\langle \mathbf{b} \rangle}. \tag{31}$$

There are some key differences between the vorticity equations (31) and (27). In the depth-averaged vorticity equation (27), there is no contribution from lateral pressure gradients but the vertical velocities at boundaries appear in the budget. On the other hand, in vorticity equation of the depth-averaged flow (31), the curl of the pressure gradient term does not vanish due to the presence of variable topography and free surface undulations, and there are no vertical velocity terms associated with vortex stretching. The remaining terms also possess some differences due to the different mathematical formulation.

The depth averaged vorticity equation (27) is a natural approach to a two-dimensional vorticity analysis. However, we do not compute a layerwise vorticity budget in MOM6 so that diagnosing this budget is not convenient. Rather, the terms appearing in the vorticity equation of the depth-averaged flow (31) are more readily diagnosed. But when working with this budget we must be aware of some limitations. In particular, the vorticity equation for the depth-averaged velocity (31) contains the JEBAR term (joint effect of baroclinicity and relief), which is the second term on the RHS of equation (31)

$$\mathrm{JEBAR} = -\frac{1}{\rho_o} \nabla \wedge \overline{\langle \nabla p \rangle}. \tag{32}$$

As detailed in (*Mertz and Wright*, 1992), JEBAR is a "correction" to the vortex-stretching arising with variable topography, and JEBAR does not represent any physical process. Furthermore, the JEBAR term is expected to be opposite in sign but of similar magnitude to the first term on the RHS in equation (31). Thus, these two terms compensate for each other. Correspondingly, it can be difficult to accurately diagnose the JEBAR term, which can lead to misleading interpretations (*Mertz and Wright*, 1992; *Cane et al.*, 1998). For this reason it may be more appropriate to treat the first two terms on the RHS in equation (31) as a single term for comparison against other terms in the budget.

4.3 Vorticity of the depth-integrated flow

Another approach for vorticity budget analysis is to study the vorticity of the depth-integrated velocity. This approach offers a middle ground between the depth averaged vorticity and the vorticity of the depth averaged velocity. In particular, there is no JEBAR term in this approach.

To derive the vorticity budget of the depth-integrated flow, we first vertically integrate the momentum equation (21a) from the ocean bottom, $z=-H(x,y)$, to the sea surface, $z=\eta(x,y,t)$),

$$\int_{-H}^{\eta} \partial_t \mathbf{u}\, \mathrm{d}z = -f\hat{\mathbf{z}}\wedge\int_{-H}^{\eta}\mathbf{u}\,\mathrm{d}z - \frac{1}{\rho_o}\int_{-H}^{\eta}\nabla p\,\mathrm{d}z + \frac{\boldsymbol{\tau}^{(\mathrm{top})}-\boldsymbol{\tau}^{(\mathrm{bot})}}{\rho_o} + \int_{-H}^{\eta}\mathbf{a}\,\mathrm{d}z + \int_{-H}^{\eta}\mathbf{b}\,\mathrm{d}z. \tag{33}$$

We now introduce the shorthand

$$\mathscr{U}_t = \int_{-H}^{\eta}\partial_t\mathbf{u}\,\mathrm{d}z \quad \text{and} \quad \mathscr{A} = \int_{-H}^{\eta}\mathbf{a}\,\mathrm{d}z \quad \text{and} \quad \mathscr{B} = \int_{-H}^{\eta}\mathbf{b}\,\mathrm{d}z, \tag{34}$$

and make use of Leibniz's rule on the pressure gradient term to render

$$\mathscr{U}_t = -f\hat{\mathbf{z}}\wedge\int_{-H}^{\eta}\mathbf{u}\,\mathrm{d}z - \frac{1}{\rho_o}\nabla\left[\int_{-H}^{\eta}p\,\mathrm{d}z\right] + p^{(\mathrm{top})}\nabla\eta + p^{(\mathrm{bot})}\nabla H + \frac{\boldsymbol{\tau}^{(\mathrm{top})}-\boldsymbol{\tau}^{(\mathrm{bot})}}{\rho_o} + \mathscr{A} + \mathscr{B}. \tag{35}$$

Here, $p^{(\mathrm{top})}$ and $p^{(\mathrm{bot})}$ are pressures at the surface and bottom of the ocean, and the terms $p^{(\mathrm{top})}\nabla\eta + p^{(\mathrm{bot})}\nabla H$ are pressure form stresses at the ocean surface and ocean bottom. We now take the curl of this equation and obtain

$$\nabla\wedge\mathscr{U}_t = -\nabla\wedge\left(f\hat{\mathbf{z}}\wedge\int_{-H}^{\eta}\mathbf{u}\,\mathrm{d}z\right) - \frac{1}{\rho_o}\nabla\wedge\left(\nabla\int_{-H}^{\eta}p\,\mathrm{d}z - p^{(\mathrm{top})}\nabla\eta - p^{(\mathrm{bot})}\nabla H\right) + \nabla\wedge\frac{\boldsymbol{\tau}^{(\mathrm{top})}-\boldsymbol{\tau}^{(\mathrm{bot})}}{\rho_o} + \nabla\wedge\mathscr{A} + \nabla\wedge\mathscr{B}, \tag{36a}$$

$$= -\beta\int_{-H}^{\eta}v\,\mathrm{d}z - f\nabla\cdot\int_{-H}^{\eta}\mathbf{u}\,\mathrm{d}z + \frac{J(p^{(\mathrm{bot})},H)}{\rho_o} + \frac{J(p^{(\mathrm{top})},\eta)}{\rho_o} + \nabla\wedge\frac{\boldsymbol{\tau}^{(\mathrm{top})}-\boldsymbol{\tau}^{(\mathrm{bot})}}{\rho_0} + \nabla\wedge\mathscr{A} + \nabla\wedge\mathscr{B}, \tag{36b}$$

where we split the curl of the linear Coriolis term into the first two terms on the RHS. We can further massage the second term on the RHS by making use of volume conservation for a vertical column of Boussinesq fluid to write

$$\nabla\cdot\int_{-H}^{\eta}\mathbf{u}\,\mathrm{d}z = \frac{Q_m}{\rho_o} - \partial_t\eta, \tag{37}$$

which then leads to the vorticity budget for the depth-integrated flow

$$\beta\int_{-H}^{\eta}v\,\mathrm{d}z = \frac{J(p^{(\mathrm{bot})},H)}{\rho_o} + \frac{J(p^{(\mathrm{top})},\eta)}{\rho_o} - f\frac{Q_m}{\rho_o} + f\,\partial_t\eta - \nabla\wedge\mathscr{U}_t + \nabla\wedge\frac{\boldsymbol{\tau}^{(\mathrm{top})}-\boldsymbol{\tau}^{(\mathrm{bot})}}{\rho_0} + \nabla\wedge\mathscr{A} + \nabla\wedge\mathscr{B}. \tag{38}$$

Note that many climate models impose a uniform pressure at the ocean surface so that

$$J(p^{(\mathrm{top})},\eta) = 0, \tag{39}$$

which leads to the time averaged balance

$$\beta\overline{\int_{-H}^{\eta}v\,\mathrm{d}z} = \overline{\frac{J(p^{(\mathrm{bot})},H)}{\rho_o}} - f\,\overline{\frac{Q_m}{\rho_o}} + f\,\overline{\partial_t\eta} - \nabla\wedge\overline{\mathscr{U}_t} + \nabla\wedge\frac{\boldsymbol{\tau}^{(\mathrm{top})}-\boldsymbol{\tau}^{(\mathrm{bot})}}{\rho_0} + \nabla\wedge\overline{\mathscr{A}} + \nabla\wedge\overline{\mathscr{B}}. \tag{40}$$

As mentioned earlier, an advantage of using the formulation (40) (vorticity of the depth integrated flow) rather than equation (31) (vorticity of the depth averaged flow) is that JEBAR term does not appear in equatio (40). Instead, the bottom pressure torque is present

$$\mathrm{BPT} = \frac{J(p^{(\mathrm{bot})},H)}{\rho_o}. \tag{41}$$

If the bottom flow is geostrophic, then this term is equal to the vertical vortex stretching due to geostrophic flow at the ocean bottom. This approach is found to be helpful in understanding the role of mesoscale eddies and topography in the North Atlantic Ocean (see e.g. *Hughes and De Cuevas*, 2001; *Yeager*, 2015). We mainly focus on this formulation in the following discussion.

5 Diagnosing vorticity budget terms in MOM6

MOM6 is equipped with online diagnostics sufficient for an offline computation of individual terms in the vorticity equations (40) and (31). We do so by making use of the online depth-integrated and depth-averaged velocity budget diagnostics in MOM6 as listed in Table 2. We then take the curl of these terms offline to obtain the corresponding vorticity budget terms. As the model does not fully manifest the continuum identities, such as Leibniz's rule, it is useful to work directly with the model velocity diagnostic rather than the massaged forms developed in the continuum. Details are shown in Table 3.

Term	Relevant Diagnostic Calculations
$\int_{-H}^{\eta} v\,\mathrm{d}z$	`vmo_2d` / $(\rho_o \Delta x)$, where Δx and ρ_o are the zonal grid spacing and reference density
Q_m	`wfo` or `PRCmE`
$\partial_t \eta$	compute using SSH snapshots at start and end times of time-interval chosen for averaging
$\nabla \wedge \mathscr{U}_t$	$\partial_x [D \times$ `hf_dvdt_2d`$] - \partial_y [D \times$ `hf_dudt_2d`$]$
$\nabla \wedge \boldsymbol{\tau}_s$	$\partial_x \left[\texttt{tauy}\right] - \partial_y [\texttt{taux}]$
$\nabla \wedge \boldsymbol{\tau}_b$	$\partial_x \left[\texttt{tauy\_bot}\right] - \partial_y [\texttt{taux\_bot}]$
$\nabla \wedge \mathscr{A}$	$\partial_x \left[\texttt{intz\_rvxu\_2d} + \texttt{intz\_gKEv\_2d}\right] - \partial_y \left[\texttt{intz\_rvxv\_2d} + \texttt{intz\_gKEu\_2d}\right]$ + vertical remap contri.
$\nabla \wedge \mathscr{B}$	$\partial_x [\texttt{intz\_diffv\_2d}] - \partial_y [\texttt{intz\_diffu\_2d}]$

Table 3: Method for the computations of vorticity budget terms using depth-integrated momentum budget diagnostics. The contribution from remapping in $\nabla \wedge \mathscr{A}$ can be computed as discussed in momentum budget diagnostics. Moreover, terms in equation (31) can be computed using depth-averaged momentum budget terms.

Diagnosis of the bottom pressure torque (BPT) requires some care since the model does not satisfy a discrete version of Leibniz's rule. From the development in Section 4.3, we write

$$\frac{J(p^{(\mathrm{bot})}, H)}{\rho_o} = -\nabla \wedge \left[f\hat{\mathbf{z}} \wedge \int_{-H}^{\eta} \mathbf{u}\,\mathrm{d}z + \frac{1}{\rho_o}\int_{-H}^{\eta} \nabla p\,\mathrm{d}z \right] + \beta \int_{-H}^{\eta} v\,\mathrm{d}z + f\frac{Q_m}{\rho_o} - f\partial_t \eta, \tag{42}$$

with rearrangement leading to the diagnostic equation

$$\begin{aligned} \frac{J(p^{(\mathrm{bot})}, H)}{\rho_o} &= \partial_x \left[\texttt{intz\_CAv\_2d} - \texttt{intz\_rvxu\_2d} - \texttt{intz\_gKEv\_2d}\right] \\ &- \partial_y \left[\texttt{intz\_CAu\_2d} - \texttt{intz\_rvxv\_2d} - \texttt{intz\_gKEu\_2d}\right] \\ &+ \partial_x [\texttt{intz\_PFv\_2d} + \texttt{intz\_v\_BT\_accel\_2d}] - \partial_y [\texttt{intz\_PFu\_2d} + \texttt{intz\_u\_BT\_accel\_2d}] \\ &+ \frac{\beta}{\rho_o \Delta x} \times \texttt{vmo\_2d} + \frac{f}{\rho_o} \times \texttt{wfo} - f\partial_t \eta. \end{aligned} \tag{43}$$

This approach was found to be most suitable because the terms on the RHS in the first three lines in equation (43) can be unrealistically large. In general, we expect a significant cancellation between the zonal and meridional gradients when we compute the curl of planetary vorticity advection term, and we expect to obtain $\beta \times V$ (see first two terms on the RHS in equation (36b)). A similar situation is expected in the curl of depth-integrated pressure gradient term. However, this expectation does not seem to follow in individual curl operations in equation (43), but the cancellation happens when we take the sum of the curls of Coriolis advection and pressure gradient terms (see Figure 3). This behavior could be related to the numerical handling of the momentum terms in MOM6 and it requires further analysis. Thus, we opt to use relation (43) to compute the BPT.

In Figure 4 we show the vorticity budget terms from equation (40). The largest terms appear to be the BPT and curl of the depth-integrated nonlinear advection ($\nabla \times \overline{\mathscr{A}}$). These two terms largely cancel and the net is very close to $\beta \overline{V}$. We compare these MOM6 results with those from a 2 km simulation with the terrain-following model CROCO (*Corre et al.*, 2020). We are encouraged with the MOM6 diagnostic since the patterns largely agree (compare figures 4 and 5) even though the diagnostic and prognostic methods are very different.

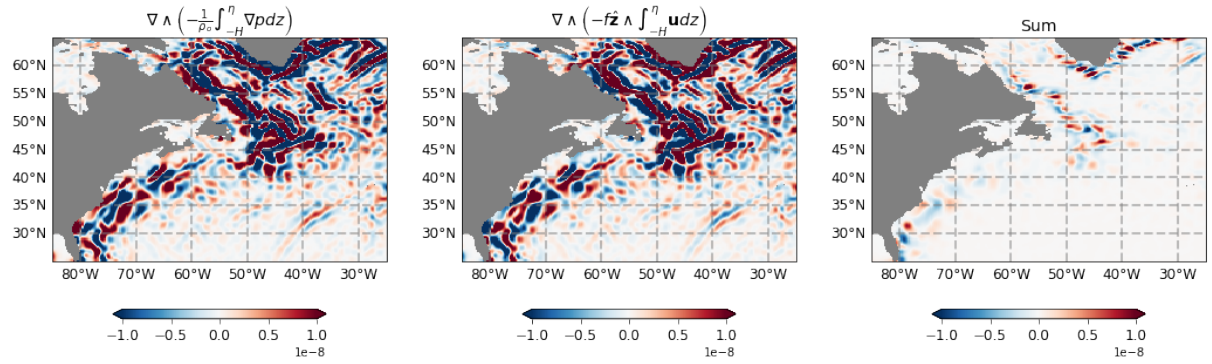

Figure 3: Curl of depth-integrated Coriolis advection term (left panel), curl of depth-integrated pressure gradient term (middle panel), and the sum of the two fields (right panel) using a 1/4° global coupled MOM6 simulation. All fields (in m s^{-2}) are spatially smoothed using a Gaussian filter kernel of radius 1°.

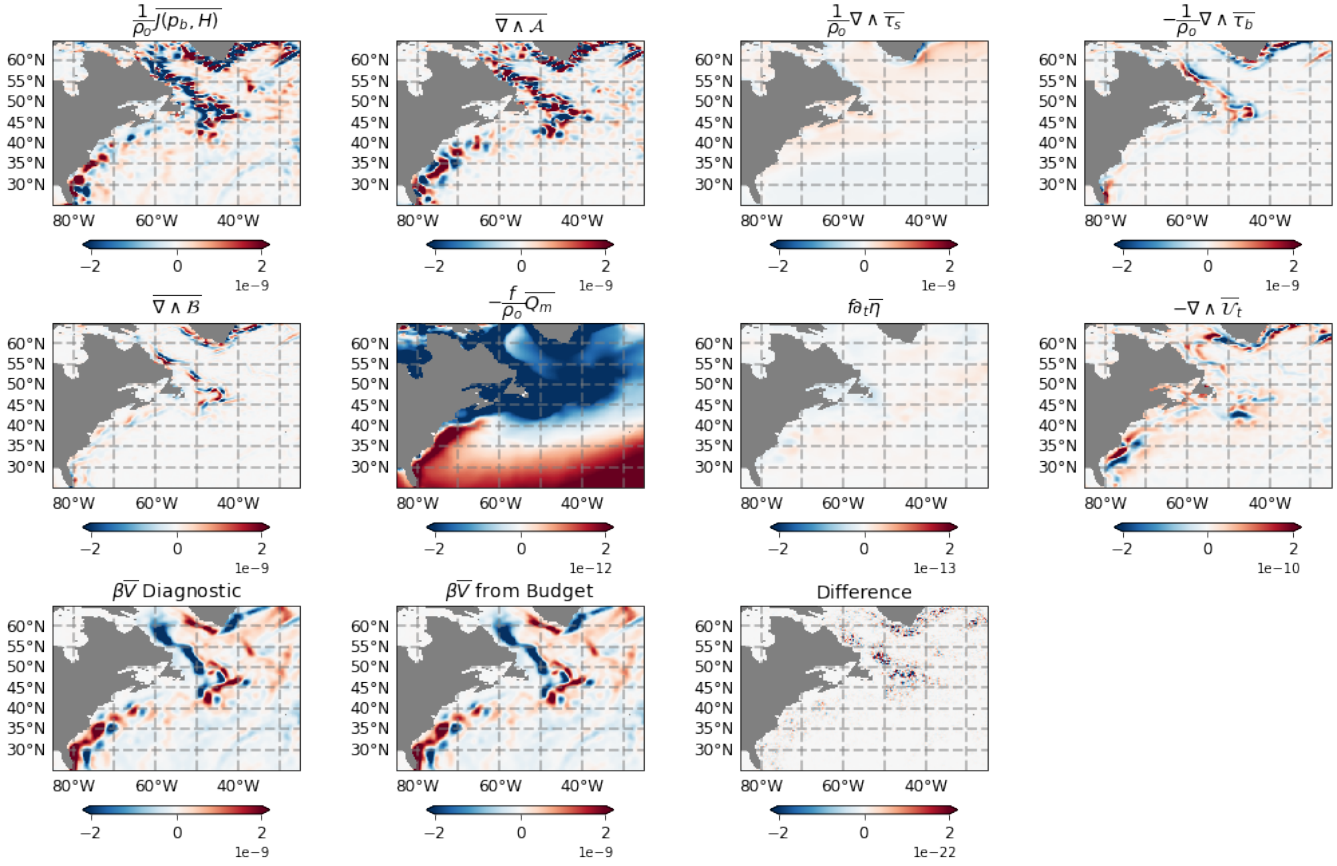

Figure 4: The first two rows show the budget terms (units are in m s^{-2}) from the vorticity equation (40) using a 1/4° global MOM6 simulation (fields averaged over 5 years). The computation details for each term are given in Table 3. In the third row, the $\beta\overline{V}$ diagnostic in the bottom left panel is computed directly from model output. It is compared against the sum of all terms in the first two rows (middle bottom panel) with the difference between the two more than 10 orders of magnitude smaller (bottom right panel). All fields are spatially smoothed using a Gaussian filter kernel of radius 1°.

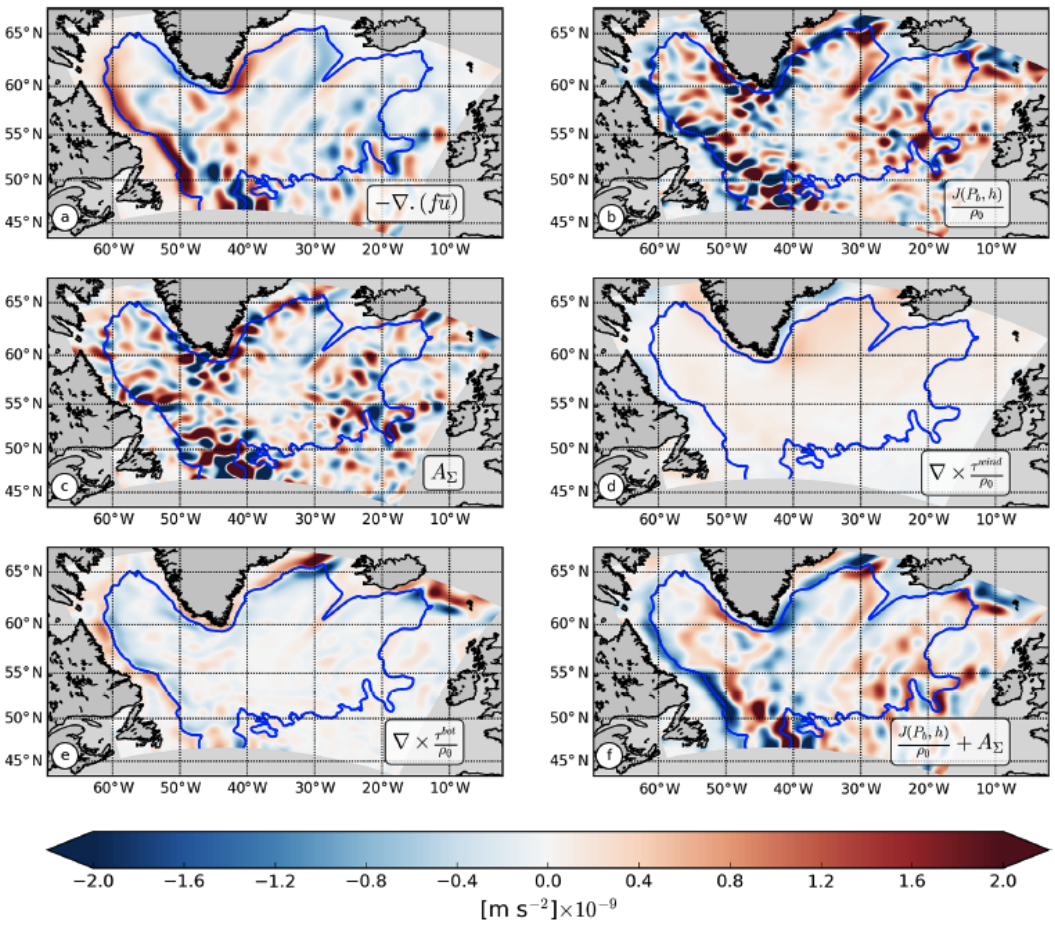

Figure 5: Vorticity budget terms from 2 km resolution CROCO model simulation (*Corre et al.*, 2020). All fields are spatially smoothed using a kernel of radius 1°.

A Examples from a hierarchy of channel models

In developing the online diagnostics and offline scripts, we found it useful to examine results from the following hierarchy of channel test cases. For each test we diagnose the terms using the model's native vertical grid since mapping to non-native vertical grids has yet to be coded for the velocity diagnostics.[5]

1. SINGLE SHALLOW WATER LAYER DRIVEN BY WIND: This adiabatic and single layer experiment includes bottom friction and bottom topography and is driven by wind. There is no vertical remapping so that the dia-surface velocity vanishes, $w^{(\dot{s})} = 0$. Most of the other terms in the equation of motion are present, thus allowing us to locate them in the code and ensure that this very simple test case balances.

2. TWO-LAYER WIND-DRIVEN SHALLOW WATER: This configuration is also adiabatic so that $w^{(\dot{s})} = 0$ and there is no contribution from vertical remapping. With two layers encounter diagnostics in the presence of a barotropic/baroclinic time stepping split. This test revealed many early problems with the diagnostics since the time splitting algorithm in MOM6 is rather tricky.

3. CONTINUOUSLY STRATIFIED z^*: This configuration is identical to the above and yet it uses the continuously stratified z^* vertical coordinate with a full suite of horizontal and vertical friction operators. In this case

[5]Tracer diagnostics have been enabled on native and remapped grids, but that work has not been done for velocity diagnostics.

$w^{(\hat{s})} \neq 0$ so we need to write analysis code to diagnose the associated contribution to the velocity equation. This test includes all terms in the velocity equation.

4. CONTINUOUSLY STRATIFIED ρ_{2000}: This configuration follows the previous one yet uses a continuously stratified ρ_{2000} vertical coordinate. Ideally this test should reveal no new issues relative to the z^* case, but it is important to run this test to be sure.

A.1 Two-layer shallow water model budgets

We here exhibit terms from the velocity equation (1) in the two-layer shallow water zonally re-entrant channel forced with a zonally uniform zonal wind stress. As expected, the dominant balance is geostrophic as seen in Figure 6. The terms in Table 1 completely close the velocity budget and the residual is just computational round-off. Note that the sum of barotropic acceleration and pressure acceleration terms is plotted in pressure force acceleration panels in Figure 6.

In Figure 7, the barotropic and depth averaged velocity tendency terms are compared. These terms are largely equal (top two rows) and the small difference is due to the derivative of the layer thickness divided by the total depth (see equation 20b).

A.2 Budgets in continuously stratified z* simulation

In Figure 9, depth-averaged momentum budget terms are shown from a continuously stratified simulation that was forced with steady zonal wind stress and surface heat and freshwater fluxes. Similar to shallow water runs, the primary balance is between the pressure gradient and Coriolis terms. Other terms are roughly an order of magnitude smaller. The residual is largest over topography, but it is tiny compared to the other individual terms. Vorticity budget terms (31) are shown in Figure 10.

Acknowledgments

We thank Alistair Adcroft, Bob Hallberg, Andrew Shao, and Marshall Ward for their patience and advice with our diagnostic code development. Maike Sonnewald provided very important feedback and encouragement throughout the development process. Hemant Khatri is sponsored through award NA18OAR4320123 from the National Oceanic and Atmospheric Administration, U.S. Department of Commerce.

References

Adcroft, A., W. Anderson, C. Blanton, M. Bushuk, C. O. Dufour, J. P. Dunne, S. M. Griffies, R. W. Hallberg, M. J. Harrison, I. Held, M. Jansen, J. John, J. P. Krasting, A. Langenhorst, S. Legg, Z. Liang, C. McHugh, B. G. Reichl, A. Radhakrishnan, T. Rosati, B. Samuels, A. Shao, R. J. Stouffer, M. Winton, A. T. Wittenberg, B. Xiang, N. Zadeh, and R. Zhang (2019), The GFDL global ocean and sea ice model OM4.0: Model description and simulation features, *Journal of Advances in Modeling the Earth System, JAMES*, doi:10.1029/2019MS001726.

Cane, M. A., V. M. Kamenkovich, and A. Krupitsky (1998), On the utility and disutility of JEBAR, *Journal of Physical Oceanography, 28*(3), 519–526.

Corre, M. L., J. Gula, and A.-M. Tréguier (2020), Barotropic vorticity balance of the North Atlantic subpolar gyre in an eddy-resolving model, *Ocean Science, 16*(2), 451–468.

Hughes, C. W., and B. A. De Cuevas (2001), Why western boundary currents in realistic oceans are inviscid: A link between form stress and bottom pressure torques, *Journal of Physical Oceanography, 31*(10), 2871–2885.

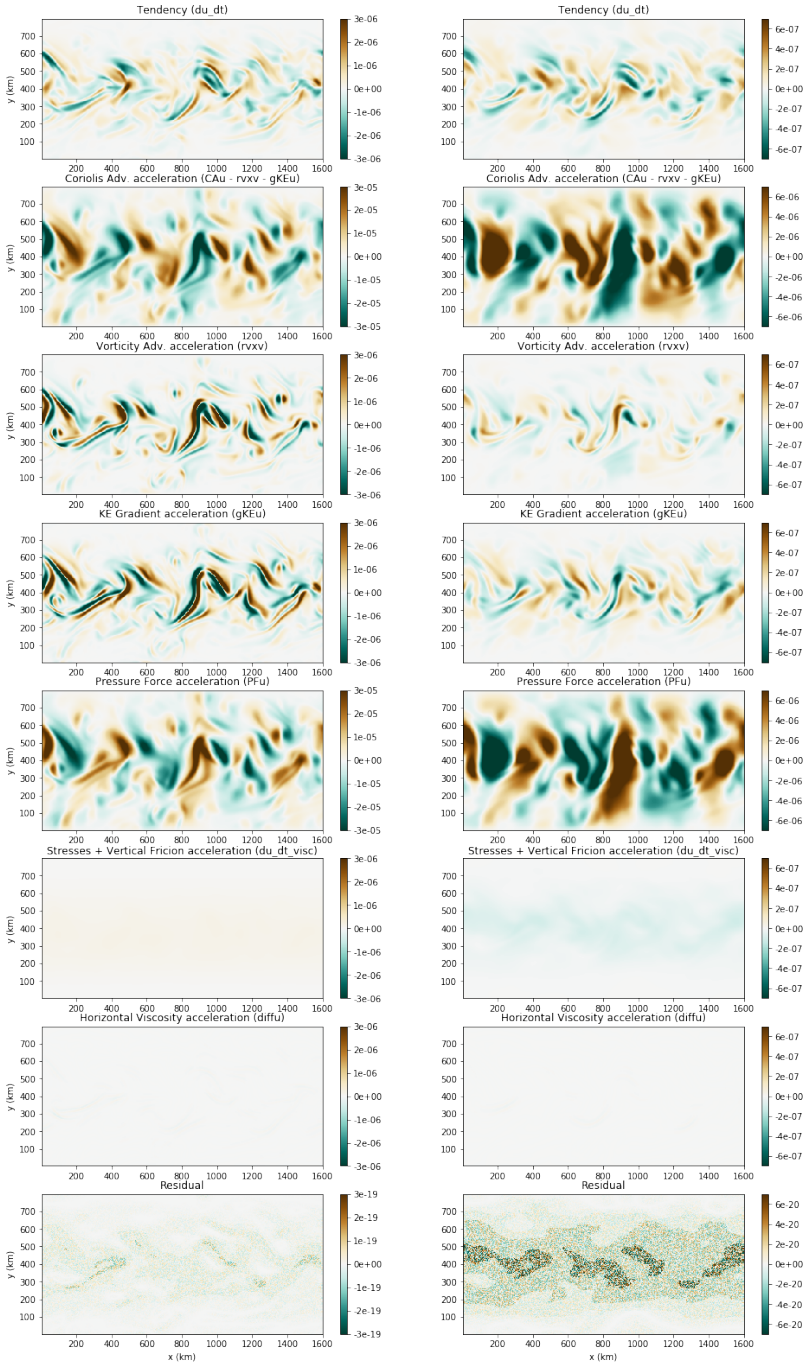

Figure 6: Layer-wise zonal momentum budget (left and right panels are for the top and bottom layers) obtained using snapshots of different diagnostics (units are in m s^{-2}). The balances also holds for time-averaged diagnostics. Note that the colorbar range is different in the different panels.

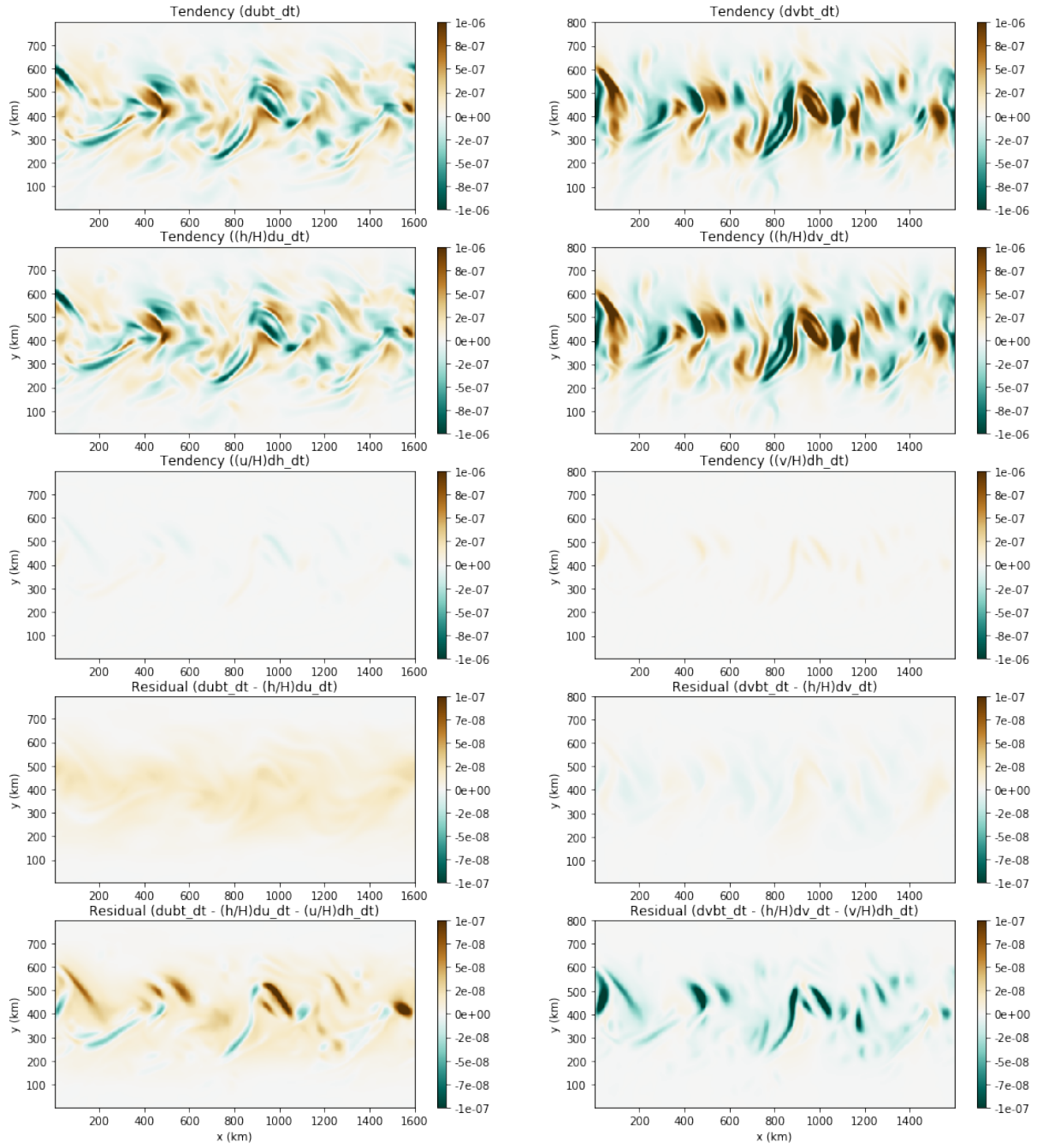

Figure 7: Barotropic velocity and depth-averaged velocity tendency terms (left and right panels are for the zonal and meridional velocities). Note that the colorbar range is different in different panels (units are in m s^{-2}).

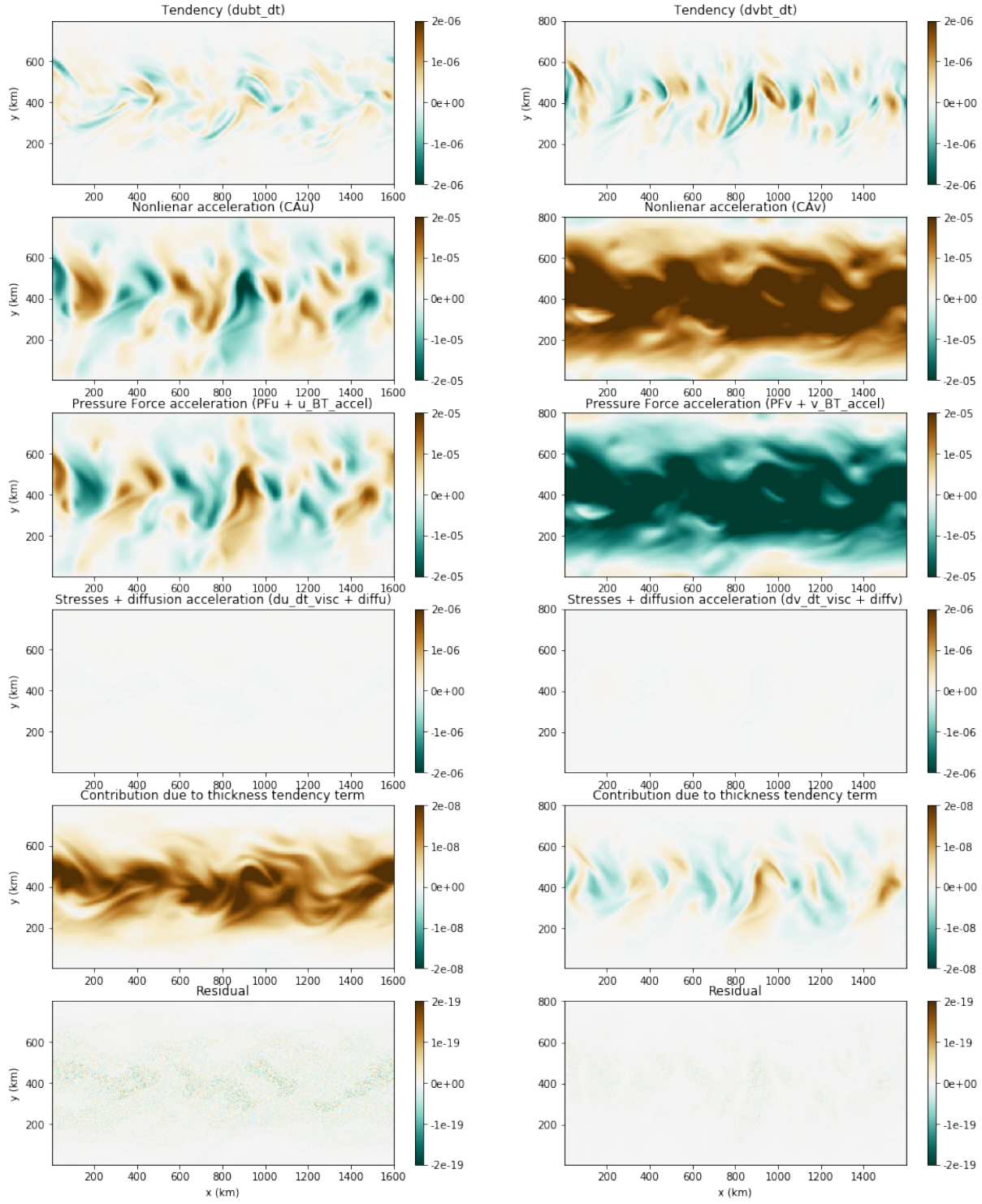

Figure 8: Barotropic momentum budget (left and right panels are for the zonal and meridional momentum) obtained using snapshots of different diagnostics. Note that the colorbar range is different in different panels (units are in m s^{-2}).

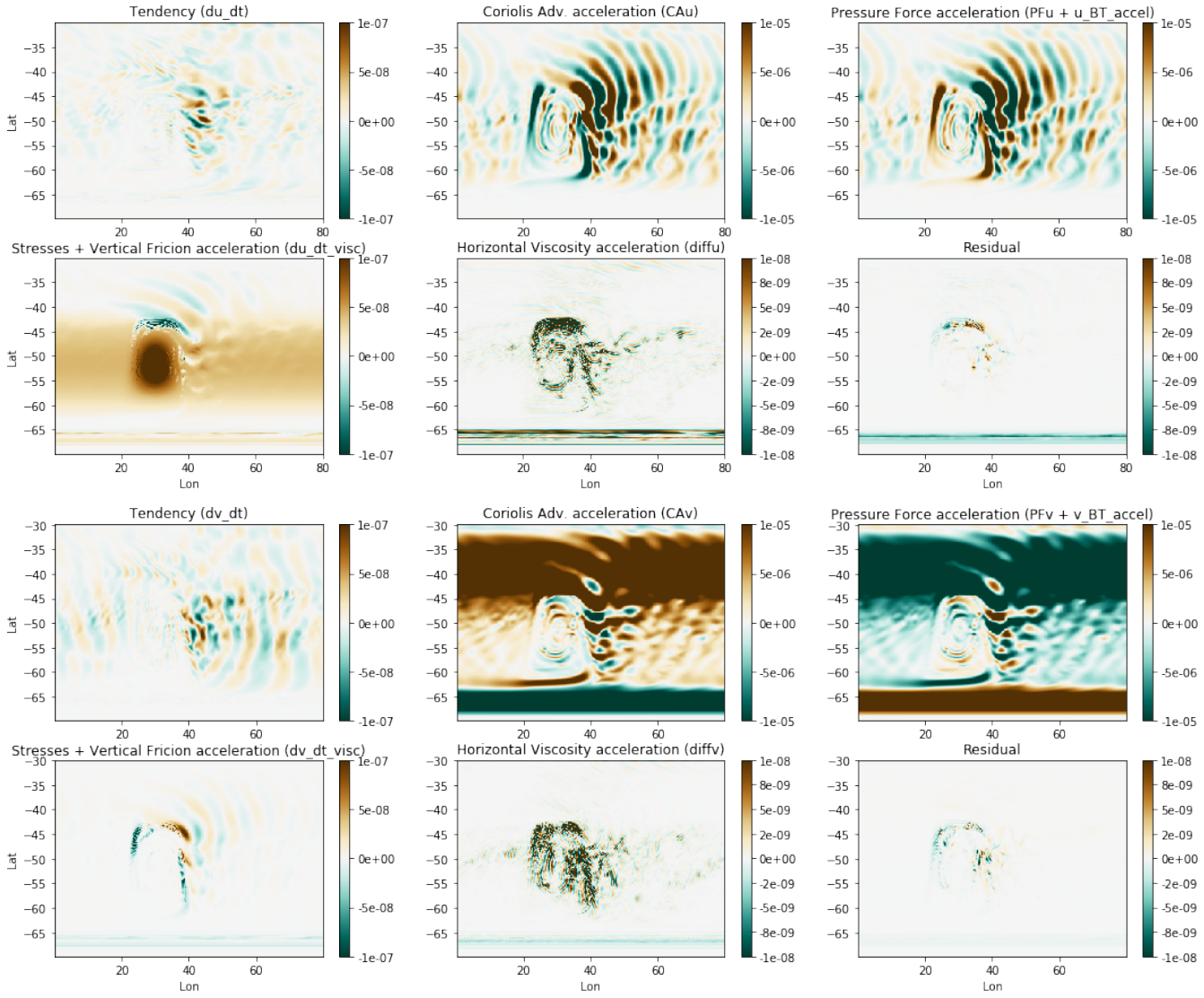

Figure 9: Terms depth-averaged in zonal (top two rows) and meridional momentum (bottom two rows) budgets (table 2) obtained using monthly-averaged diagnostics from an zonally re-entrant idealized channel simulation. Note that the colorbar range is different in different panels (units are in m s^{-2}).

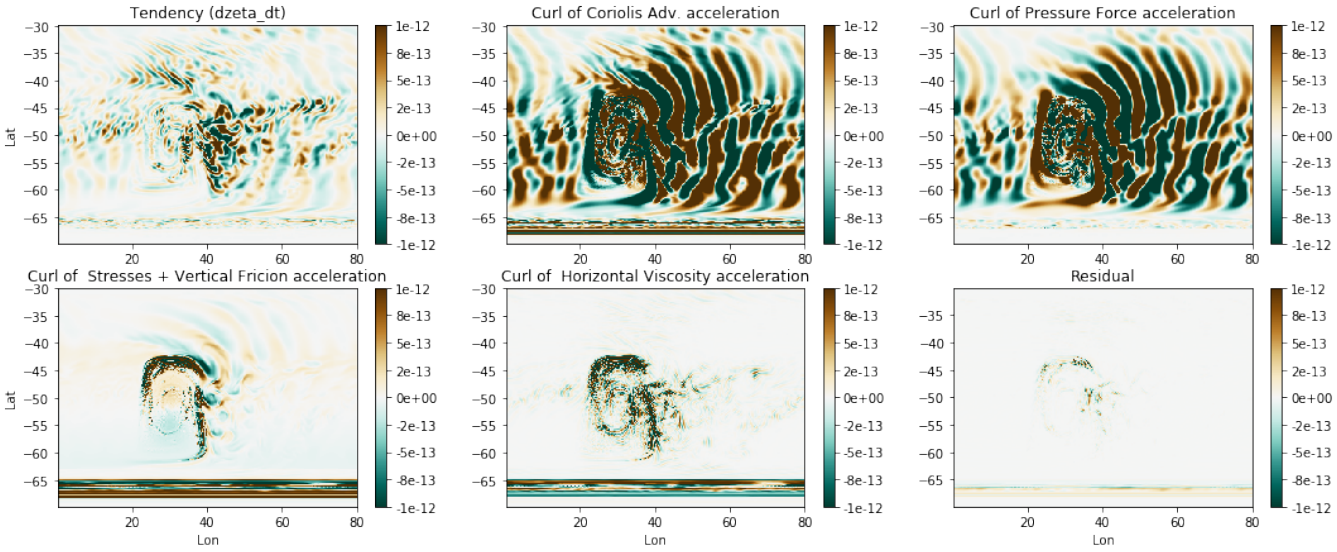

Figure 10: Terms (units are in s^{-2}) in in vorticity budget of the depth-averaged flow (31) obtained by taking curl of depth-averaged momentum budget terms from an zonally re-entrant idealized channel simulation.

Mertz, G., and D. G. Wright (1992), Interpretations of the JEBAR term, *Journal of Physical Oceanography*, *22*(3), 301–305.

Yeager, S. (2015), Topographic coupling of the Atlantic overturning and gyre circulations, *Journal of Physical Oceanography*, *45*(5), 1258–1284.